Interpolation of 2-D Vector Data Using Constraints from Elasticity

David T. Sandwell
Scripps Institution of Oceanography, UC San Diego, La Jolla, CA

Paul Wessel
SOEST, University of Hawaii at Mānoa, Honolulu, HI

Citation:
Sandwell, D. T., and P. Wessel (2016), Interpolation of 2-D vector data using constraints from elasticity, Geophys. Res. Lett., 43, doi:10.1002/2016GL070340.

Key points: interpolation of vector data, GPS gridding, Green's functions for 2-D elastic body

Abstract
We present a method for interpolation of sparse two-dimensional vector data. The method is based on the Green's functions of an elastic body subjected to in-plane forces. This approach ensures elastic coupling between the two components of the interpolation. Users may adjust the coupling by varying Poisson's ratio. Smoothing can be achieved by ignoring the smallest eigenvalues in the matrix solution for the strengths of the unknown body forces. We demonstrate the method using irregularly distributed GPS velocities from southern California. Our technique has been implemented in both GMT and MATLAB®.

Introduction

Interpolation of randomly located scalar data onto a uniform grid is commonly performed using the finite-difference, multigrid, minimum curvature method [*Briggs,* 1974; *Swain*, 1976; *Smith and Wessel,* 1990] or the direct biharmonic spline method [*Sandwell,* 1987; *Wessel and Bercovici,* 1998]. The multigrid minimum curvature approach is extremely efficient and can handle large data sets of perhaps a billion data points, but suffers from slow numerical convergence. The direct biharmonic spline approach is more flexible and can interpolate data with differing uncertainties but is limited to only a few thousand points because an *N*-data by *N*-data matrix inversion is required. Moreover, the inversion usually requires some numerical stabilization to achieve a smooth result. The basic approach is to apply vertical point loads to a thin elastic sheet at the locations of the data constraints. The

strengths of these forces are then adjusted through a least squares inversion such that the deformed sheet matches the data points within their uncertainties. Then the deformation, or its derivatives, can be calculated anywhere within the boundaries of the data. The Green's function for the response of a thin elastic sheet to a point load at (x_o, y_o) is simply $\phi(\vec{r}) = r^2[\ln(r) - 1]$ where $\vec{r} = (x - x_o, y - y_o)$ [*Sandwell,* 1987]. *Wessel and Bercovici* [1998] extended the method to include in-plane tension, which damps the undesirable overshoots of the elastic sheet. In this case the Green's function is slightly more complicated, i.e., $\phi(\vec{r}) = K_o(pr) + \ln(pr)$, where K_o is the zero order, modified Bessel function of the second kind and *p* is related to the prescribed tension factor.

Here we investigate a similar Green's function approach for interpolation of 2-D vector data. This is not a new idea. *Haines and Holt* [1993] and *Haines et al.,* [2015] proposed using a 2-D elastic model to provide coupling between the two horizontal velocity components of GPS models. The basic approach is similar to the biharmonic spline interpolation approach. One imposes vector forces at the data locations. These forces deform the elastic body, resulting in a vector deformation field. The strengths of the force vectors are adjusted until velocities match the vector data. *Haines et al.,* [2015] used a finite element modeling approach where element nodes are placed at the data locations to compute the Green's functions and then used a least-squares approach to adjust the forces to match the data. Here we replace the finite element computations with analytic Green's functions for the in-plane response of a 2-D elastic body to in-plane forces. This greatly simplifies the computations and allows for the analytic calculation of deformation gradients (i.e., the strain tensor). Moreover, by adjusting Poisson's ratio the strain field can be tuned to extremes such as incompressible (1.0), typical elastic (0.5) or even a value of -1 that basically removes the elastic coupling of vector interpolation.

Green's Functions

We wish to calculate the 2-D displacement vector $\vec{u}(x,y) = u(x,y)\hat{i} + v(x,y)\hat{j}$ due to a 2-D vector in-plane body force. *Haines et al.,* [2015] developed the quasi-static force balance equations in 2-D as

$$\begin{aligned}\left(\frac{2}{1-\nu}\right)\frac{\partial^2 u}{\partial x^2}+\left(\frac{2\nu}{1-\nu}\right)\frac{\partial^2 v}{\partial x\,\partial y}+\frac{\partial^2 u}{\partial y^2}+\frac{\partial^2 v}{\partial x\,\partial y}&=\frac{-f_x}{\mu}\delta(x)\delta(y)\\ \frac{\partial^2 u}{\partial x\,\partial y}+\frac{\partial^2 v}{\partial x^2}+\left(\frac{2\nu}{1-\nu}\right)\frac{\partial^2 u}{\partial x\,\partial y}+\left(\frac{2}{1-\nu}\right)\frac{\partial^2 v}{\partial y^2}&=\frac{-f_y}{\mu}\delta(x)\delta(y)\end{aligned}, \tag{1}$$

where ν is Poisson's ratio, μ is the shear modulus, and (f_x, f_y) is the force vector. The units are force per distance and forces are applied at a point using the 2-D delta function $\delta(x)\delta(y)$. This problem is most easily solved by taking the 2-D Fourier transform of (1). The transformed equations become

$$\begin{bmatrix}\left(\frac{2}{1-\nu}\right)k_x^2+k_y^2 & \left(\frac{1+\nu}{1-\nu}\right)k_xk_y\\ \left(\frac{1+\nu}{1-\nu}\right)k_xk_y & \left(\frac{2}{1-\nu}\right)k_y^2+k_x^2\end{bmatrix}\begin{bmatrix}U(\vec{k})\\ V(\vec{k})\end{bmatrix}=\frac{1}{4\pi^2\mu}\begin{bmatrix}f_x\\ f_y\end{bmatrix}. \tag{2}$$

where k_x and k_y are wavenumbers (1/wavelength). To determine the response from a point force we need to invert this set of equations and take the inverse 2-D Fourier transform of the result. The matrix inverse is

$$\begin{bmatrix}U(\vec{k})\\ V(\vec{k})\end{bmatrix}=\frac{1}{8\pi^2\mu k_r^4}\begin{bmatrix}2k_r^2-(1+\nu)k_x^2 & -(1+\nu)k_xk_y\\ -(1+\nu)k_xk_y & 2k_r^2-(1+\nu)k_y^2\end{bmatrix}\begin{bmatrix}f_x\\ f_y\end{bmatrix} \tag{3}$$

where $k_r^2=k_x^2+k_y^2$. Note that in the special case of a Poisson's ratio of -1 the solution simplifies to

$$\begin{bmatrix}U(\vec{k})\\ V(\vec{k})\end{bmatrix}=\frac{1}{4\pi^2\mu k_r^2}\begin{bmatrix}1 & 0\\ 0 & 1\end{bmatrix}\begin{bmatrix}f_x\\ f_y\end{bmatrix} \tag{4}$$

This corresponds to interpolation with no coupling between the two velocity components and the Green's function is simply $\phi(\vec{r}) = \ln r$. Here, the two components of GPS velocities would be decoupled and interpolated separately. The general solution depends on three functions in equation 3:

$$Q(\vec{k}) = \frac{2k_r^2 - (1+\nu)k_x^2}{k_r^4}, \quad P(\vec{k}) = \frac{2k_r^2 - (1+\nu)k_y^2}{k_r^4}, \quad W(\vec{k}) = \frac{-(1+\nu)k_x k_y}{k_r^4}. \tag{5}$$

To obtain the space domain solution we will need to evaluate the 2-D inverse Fourier transform of the following four component functions:

$$\Im_2^{-1}\left[\frac{1}{k_x^2+k_y^2}\right], \quad \Im_2^{-1}\left[\frac{k_x^2}{\left(k_x^2+k_y^2\right)^2}\right], \quad \Im_2^{-1}\left[\frac{k_y^2}{\left(k_x^2+k_y^2\right)^2}\right], \quad \Im_2^{-1}\left[\frac{k_x k_y}{\left(k_x^2+k_y^2\right)^2}\right] . \tag{6}$$

The inverse transforms of these four functions are straightforward and yield

$$-\ln r, \quad \frac{1}{2}\left[\frac{y^2}{r^2} - \ln r\right], \quad \frac{1}{2}\left[\frac{x^2}{r^2} - \ln r\right], \quad -\frac{1}{2}\frac{xy}{r^2} \quad . \tag{7}$$

In the space domain the three Green's functions given by (5) can be written as

$$q(\vec{r}) = 4\ln r + (1+\nu)\left(\frac{y^2}{r^2} - \ln r\right) = (3-\nu)\ln r + (1+\nu)\frac{y^2}{r^2}$$

$$p(\vec{r}) = (3-\nu)\ln r + (1+\nu)\frac{x^2}{r^2} \tag{8}$$

$$w(\vec{r}) = -(1+\nu)\frac{xy}{r^2}.$$

We checked the Green's functions by showing they solve the original differential equation (1). This was accomplished using the computer algebra capabilities in MATLAB.

A description of the numerical approach follows. We wish to compute a smooth vector velocity field that matches a finite set of N measured vectors $u(\vec{r}_i), v(\vec{r}_i)$, where $\vec{r}_i = (x_i, y_i)$ are the locations of the vectors. This is accomplished by solving for a set of N vector body forces f_x^j, f_y^j that are applied at the locations of the velocity measurements. To determine the strength of the body forces we invert the following $2N$ by $2N$ linear system of equations:

$$\begin{bmatrix} u(\vec{r}_i) \\ v(\vec{r}_i) \end{bmatrix} = \begin{bmatrix} q(\vec{r}_i - \vec{r}_j) & w(\vec{r}_i - \vec{r}_j) \\ w(\vec{r}_i - \vec{r}_j) & p(\vec{r}_i - \vec{r}_j) \end{bmatrix} \begin{bmatrix} f_x^j \\ f_y^j \end{bmatrix} \tag{9}$$

Finally, the vector velocity field can be computed at any location using

$$\begin{aligned} u(\vec{r}) &= \sum_{j=1}^{N} \left[q(\vec{r} - \vec{r}_j) f_x^j + w(\vec{r} - \vec{r}_j) f_y^j \right] \\ v(\vec{r}) &= \sum_{j=1}^{N} \left[w(\vec{r} - \vec{r}_j) f_x^j + p(\vec{r} - \vec{r}_j) f_y^j \right] \end{aligned} . \tag{10}$$

We have implemented this approach as a new module *gpsgridder* to the Generic Mapping Tools (GMT) [*Wessel et al*., 2013]. The $2N$ by $2N$ matrix in equation 9 can be solved in a variety of ways. For the *gpsgridder* implementation we use the singular value decomposition algorithm implemented in LAPACK. The user can decide to keep all the singular values (solved by LU decomposition) or a subset which results in some smoothing of the solution. Starting at GMT release 5.3.0, the new module can be found in the supplemental "potential" package.

Application to GPS data

The 2-D velocity field derived from surface geodetic measurements is an important quantity used to measure strain localization above locked faults as well as strain accumulation in the interiors of crustal blocks. Faults that have a shallow locking will require spatial resolution of 2-3 km [*Smith and Sandwell,* 2003]. However, the typical spacing of GPS points in California is ~9 km [*Wei et al*., 2010] so the strain-rate field is not completely resolved by the GPS data. Currently there are several approaches to mapping strain rate from vector GPS data. The most accurate approaches make assumptions about the

locations, slip rates, and locking depths of the major faults [*Hearn et al.,* 2010]. These are typically based on block models. The models sometimes have a uniform strain in the block interiors to absorb the residual velocity not captured by the locked dislocations [*McCaffrey et al.,* 2013]. Another approach is to make no assumptions about the fault structure and simply do a biharmonic interpolation of each velocity component independently [*Hackl et al.,* 2009]. However this leads to suboptimal results. A distance-weighted, least-squares approach, recently developed by *Shen et al.,* [2015], provides an improved strain-rate map without using a priori information about fault locations and orientations. The interpolation approach developed in *Haines et al.,* [2015] provides coupling between the two horizontal velocity components, resulting in a more accurate interpolation of the velocity and strain field.

To illustrate the benefits of the coupled interpolation in relation to the biharmonic spline approach we begin with a realistic model for the vector velocity field for a large region surrounding the San Andreas Fault system [*Tong et al.,* 2013; 2014]. The velocity model is based on 1981 GPS velocity vectors as well as higher spatial resolution line-of-sight velocity measurements from ALOS-1 radar interferometry. The slip rates and locking depths along 41 fault segments are adjusted to match all the velocity data (Figure 1). This model results in north and east grids of velocity at 1 km spacing. A prominent feature of the model is a creeping section of the San Andreas Fault system where there is an abrupt change in velocity across the fault (Figure 1 – green box). We sample the two components of velocity at 1768 unique locations (Figure 1 – red dots) resulting in 3536 observations. We then use the biharmonic and coupled methods to interpolate over the areas of adequate data coverage and compare the interpolated velocity and strain rate grids with the "known" velocity and strain rates. The biharmonic and coupled approaches are implemented in GMT as *greenspline* and *gpsgridder*, respectively. Each program has a number of parameters that can be adjusted to achieve an optimal fit. The *greenspline* approach achieves the best fit for zero tension factor, which corresponds to biharmonic spline interpolation [*Sandwell,* 1987]. The *gpsgridder* approach has two main parameter adjustments. The first is a minimum radius factor that needs to be added to all radial differences in equations (9) and (10) to keep the Green's functions from becoming singular. After some trial and error, we found that a minimum radius of 8 km provides the best overall fit to the data; this also roughly corresponds to the mean spacing of the GPS points of ~9 km [*Wei et al.,* 2010]. The second parameter is the value of Poisson's ratio used for the interpolation. We tested a range from -1 (fully decoupled) to 0.5 (elastic) to 1.0 (incompressible). The results, provided in Table 1, show the rms misfit of the interpolated velocity and strain rate grids with respect to the starting model. We also performed the statistics for the interpolation over just the creeping section (bold in

Table 1). The rms misfits for this creeping area are larger than the rms misfits for the entire area although the optimal minimum radius is also 8 km.

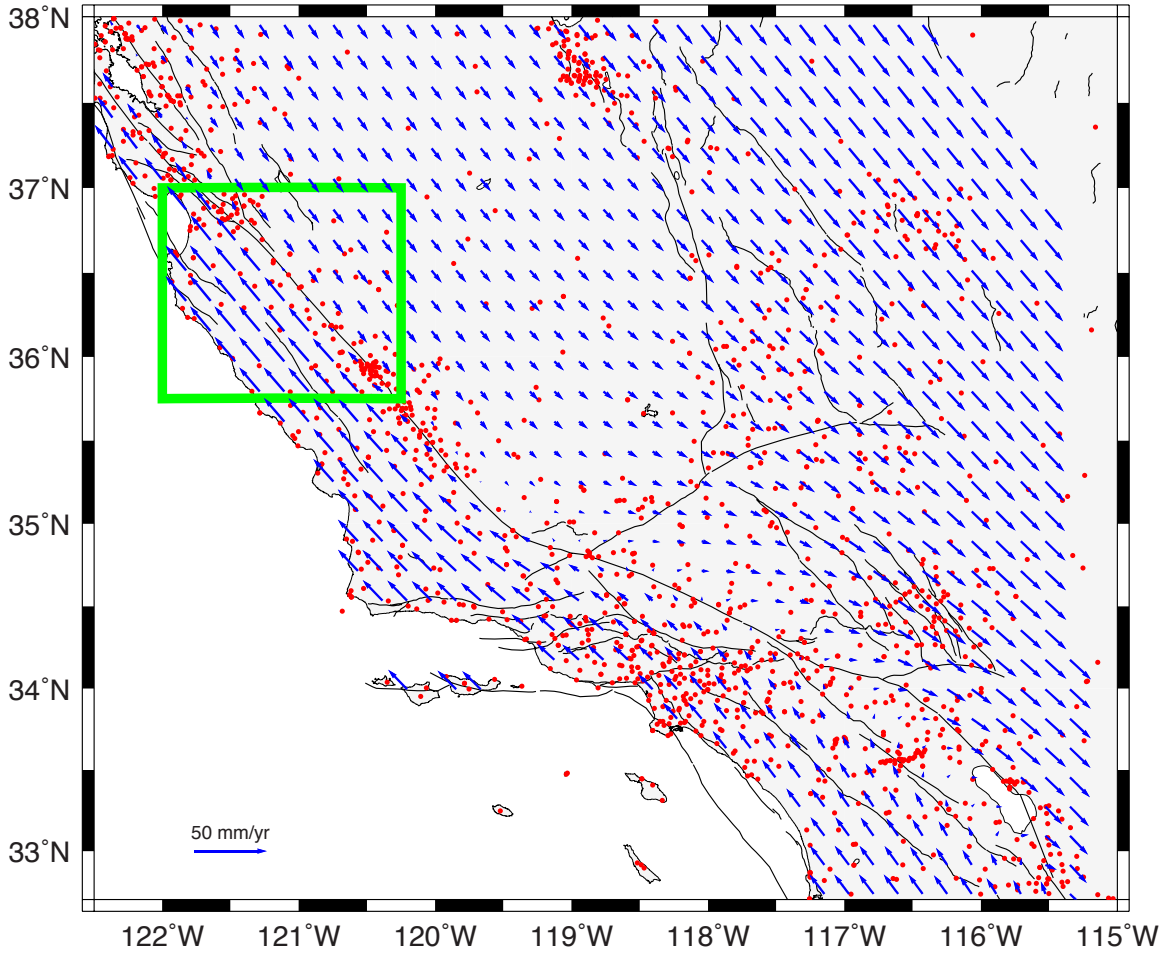

Figure 1. Velocity vectors over a large area surrounding the San Andreas Fault system based on an earthquake cycle model [*Tong et al*., 2013; 2014]. The total change in velocity across the fault system is 45 mm/yr. The red dots show locations of the GPS velocity measurements used to construct this model. We sample the model at these locations and then use various interpolation methods to re-estimate the model. The green box shows the sharp velocity change across the creeping section. These results are highlighted in Figure 2.

Table 1.

model	Poisson's ratio	minimum radius (km)	rms misfit				
			u mm/yr	v mm/yr	e_{xx} 10^{-8}/yr	e_{xy} 10^{-8}/yr	e_{yy} 10^{-8}/yr
biharmonic	-	-	0.229	0.279	3.89	1.99	4.16
(un)coupled	-1.0	8	0.186	0.223	3.48	1.99	3.83
coupled	.0	8	0.165	0.190	2.90	1.82	3.12
"	.5	8	0.162	0.171	2.66	1.82	2.81
"	1.0	8	0.863	0.894	4.91	4.29	4.89
"	.5	0	-	-	-	-	-
"	.5	2	0.281/**0.710**	0.306/**0.903**	3.77	2.38	3.87
"	.5	4	0.215/**0.509**	0.232/**0.637**	3.11	2.08	3.22
"	.5	8	0.162/**0.432**	0.171/**0.450**	2.66	1.82	2.81
"	.5	12	0.182/**0.583**	0.188/**0.577**	3.05	2.16	3.21

Optimal model parameters are highlighted in blue. Bold are rms misfit for just the creeping section shown in Figure 2.

The results for three of the most interesting cases are shown in Figure 2 where we have zoomed in on the creeping section of the fault where the interpolation is most challenging. Figure 2a shows velocity vectors from the *Tong et al*., [2014] model. The vectors are parallel to the fault and have relatively uniform length along the fault, although the direction of the vectors reverses abruptly at the fault. The first example (Figure 2b) corresponds to the biharmonic interpolation method where the east and north components of the vector velocity are interpolated independently. The residual velocity field shows large spatial scale variations in strength that results from the overshoot of the biharmonic spline. This scalloping results in a relatively large misfit for both the velocity and strain rate components. The second interpolation example (Figure 2c) corresponds to interpolation where the Poisson's ratio is -1.0. This parameter selection results in no coupling between the east and north components and the residuals are similar to the biharmonic case although somewhat smaller. The last example (Figure 2d) is the coupled interpolation with a Poisson's ratio of 0.5. The residuals are significantly smaller and show more of a random orientation reflecting the coupling between the two velocity components. This case also has a much smaller misfit in both velocity and strain rate than the two uncoupled cases.

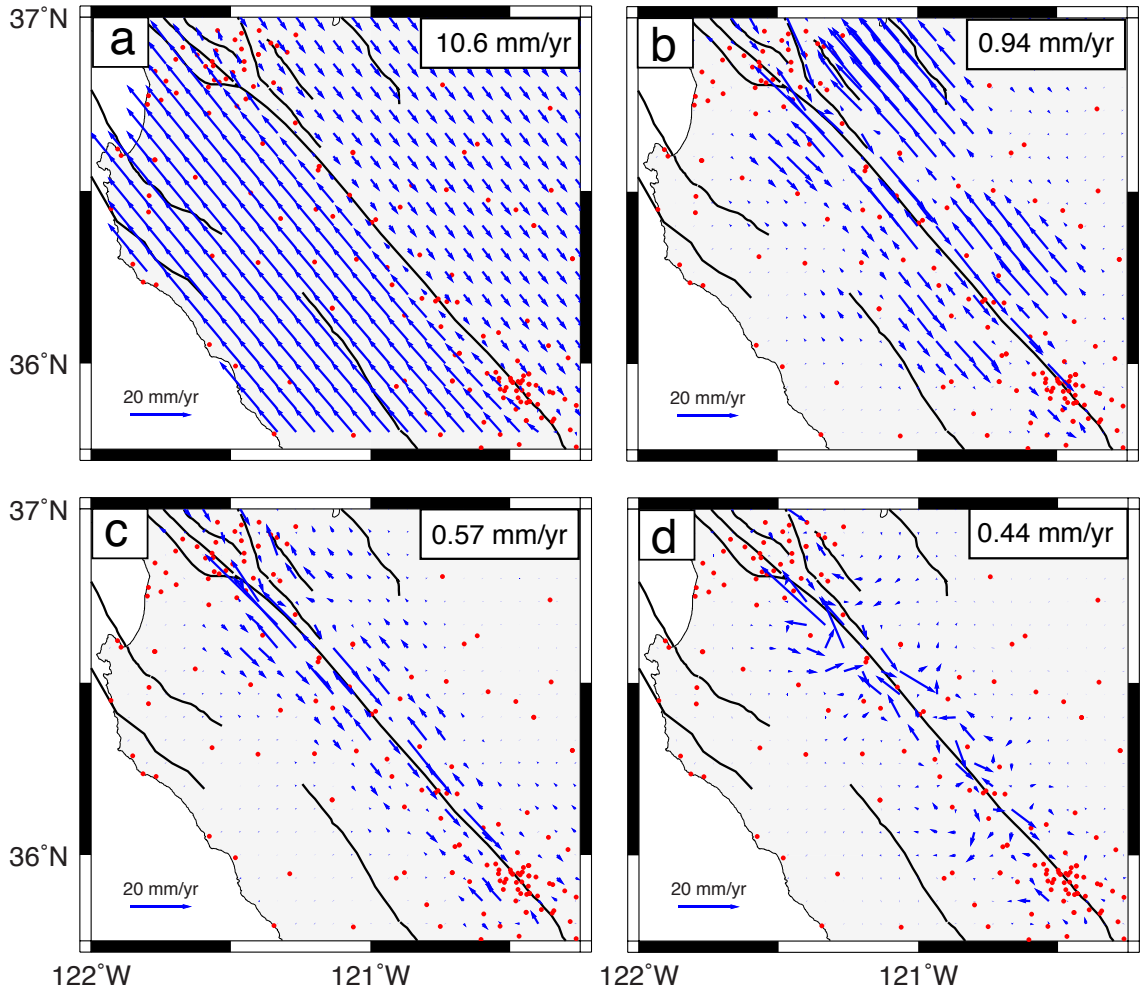

Figure 2. Velocity vectors across the creeping section of the San Andreas Fault. (a) Original *Tong et al*., [2014] model has an rms variation of 10.6 mm/yr. (b) Residual model based on biharmonic spline interpolation has an rms error of 0.94 mm/yr. (c) Residual model based on the coupled interpolation with a Poisson's ratio of -1 (no coupling between east and north velocity) has an rms error of 0.57 mm/yr. (d) Residual model based on the coupled interpolation with a Poisson's ratio of 0.5 has an rms error of 0.44 mm/yr.

One of the main applications of this method is to calculate a grid of strain rate from randomly distributed vector velocity measurements. Our analysis provides an estimate of the type of errors to expect in the second invariant of the strain rate when it is undersampled using the GPS station distribution provided in Figure 1. The original velocity model results in the strain rates shown in Figure 3a where there are areas of very high strain rate above faults that are creeping or have shallow locking depth (e.g. red areas > 500 nanostrain/yr). The model also has very low strain rate in the interiors of the blocks (e.g. blue areas < 10

nanostrain/yr). The difference between the original and recovered strain rate tensor converted to second invariant are shown in Figure 3b. Errors are small (< 3 nanostrain/yr) in areas that have adequate GPS sampling (white dots) and where the model strain rate is also small. Errors are large (100 – 1000 nanostrain/yr) in areas where the model strain rate is large and the GPS sampling is inadequate. To illustrate a couple of cases, the red arrow points to a region of high strain rate where there is also dense GPS coverage. The strain rate error in this area is quite low because of the good GPS coverage. In contrast the blue arrow points to a region of high strain rate where there is sparse GPS coverage. The strain rate error in this area is quite high because of the poor GPS coverage. Indeed this interpolation tool could be used, along with a reasonable strain rate grid, to estimate the improvement in strain rate accuracy for a prescribed GPS or InSAR data coverage.

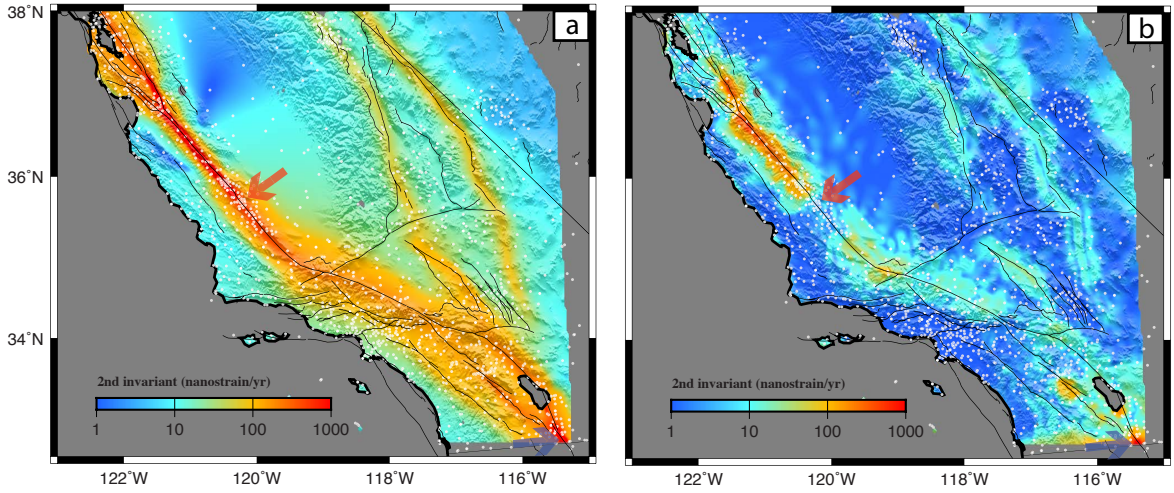

Figure 3 (a) Second invariant of 2-D strain tensor $\varepsilon_{II} = \left(\varepsilon_{xx}^2 + \varepsilon_{yy}^2 + 2\varepsilon_{xy}^2\right)^{1/2}$ derived from the *Tong et al.*, [2014] velocity grid. (b) Second invariant of the difference between the model strain rate tensor and the strain rate tensor derived from the *gpsgridder* program with a Poisson ratio of 0.5.

Discussion and Conclusions

While this method is not new, our analytic approach provides some insight into the behavior of the coupled interpolation for a wide range of Poisson's ratio. As discussed in *Haines et al.*, [1993, 2015] this approach provides improved interpolation of sparse vector data when the physics of the deforming material follows elasticity equations. There are other attributes of this approach that have not been fully discussed in the paper although they will be important for interpolation of noisy data. The first is the inversion of the set of linear equations in (9) will be numerically unstable if the ratio of the largest to smallest spacing of

vector positions becomes too great. The *gpsgridder* program automatically eliminates duplicate locations that would make the inversion exactly singular. In addition, the *blockmedian* program can be used to combine nearby measurements. The second obvious attribute not discussed above is that uncertainties are easily added to this formulation by dividing both sides of equation (9) by the standard deviations of the data. This extension is implemented in the *gpsgridder* program via the –C, –W options where the rms misfit of the model to the noisy data can be adjusted by reducing the number of eigenvalues to use for the singular value decomposition of the inversion. In the case above there were 3563 observations but tests where the number of eigenvalues was reduced to 2400 provided almost identical uncertainties. We have found that an adequate fit to real GPS data is obtained when the number of eigenvalues is ¼ the number of data points. The user will need to experiment with these paramters to find acceptable solutions to fitting the data within the uncertainties.

One other important issue not discussed here is that this approach can only interpolate thousands and not millions of data because of finite computer memory, computer precision and computer time. A practical solution to dealing with very large data sets is to assemble the data into finite size rectangular grids having 50% overlap. Data within each full subgrid are used to solve for the vector forces but the vector model velocity is only computed in the interior of each subgrid [e.g., *Sandwell,* 1987]. One final issue is that a variety of data types such as GPS vectors and 2-D tensor strain measurements could be combined in the inversion. This would require an extension of (9) to include analytical derivatives of Green functions, which are messy but not difficult.

Acknowledgements

This work was inspired by a seminar given by John Haines and Lada Dimitrovia at IGPP in December of 2015 as well as by discussions with Duncan Agnew. Duncan Agnew also provided a review of a draft manuscript that resulted in clarifications and a more complete reference list. The paper also benefited from comments from Matthias Hackl and an anonymous reviewer. The research was supported by the NSF Geoinfomatics Program (EAR-1347204) and the Southern California Earthquake Center (SCEC). SOEST publication 9837. We have implemented this method in both GMT and MATLAB and provide example data sets and programming parameters at the following ftp site (ftp://topex.ucsd.edu/pub/sandwell/strain/gpsgridder_tests.tar)

References

Briggs, I. C. (1974), Machine contouring using minimum curvature, *Geophysics*, *39*(1), 39–48.

Gradshteyn, I. S., and I. M. Ryzhik (1980), *Table of Integrals, Series, and Products*, 4th ed., Academic Press, San Diego, CA.

Hackl, M., R. Malservaisi, and S. Wdowinski (2009), Strain pattern from dense GPS networks, *Nat. Hazards Earth Syst.*, 9., 1177-1187.

Haines, A. J., and W. E. Holt (1993), A procedure for obtaining the complete horizontal motions within zones of distributed deformation from the inversion of strain rate data, *J. Geophys. Res.*, *98*, 12,057–12,082.

Haines, A. J., L. L. Dimitrova, L. M. Wallace, and C. A. Williams (2015), *Enhanced Surface Imaging of Crustal Deformation: Obtaining Tectonic Force Fields Using GPS Data*, 99 pp., Springer International Publishing, doi:10.1007/978-3-319-21578-5.

Hearn, E., K. Johnson, D. Sandwell, and W. Thatcher (2010), SCEC UCERF workshop report: http://www.scec.org/workshops/2010/gps-ucerf3/FinalReport_GPS-UCERF3Workshop.pdf,.

McCaffrey, R., King, R. W., Payne, S. J., & Lancaster, M. (2013). Active tectonics of northwestern US inferred from GPS-derived surface velocities. Journal of Geophysical Research: Solid Earth, 118(2), 709-723.

Sandwell, D. T. (1987), Biharmonic spline interpolation of Geos-3 and Seasat altimeter data, *Geophys. Res. Lett.*, *14*(2), 139–142.

Shen, Z-K, M. Wang, Y. Zeng, and F. Wang, (2015) Optimal Interpolation of Spatially Discretized Geodetic Data, *Bulletin of the Seismological Society of America, 105*, 4, 2117–2127, , doi: 10.1785/0120140247

Smith, W. H. F., and P. Wessel (1990), Gridding with continuous curvature splines in tension, *Geophysics*, *55*(3), 293–305, doi:10.1190/1.1442837.

Smith, B., and D. Sandwell (2003), Coulomb stress accumulation along the San Andreas Fault system, J. Geophys. Res., 108(B6), 2296, doi:10.1029/ 2002JB002136.

Swain, C. J. (1976), A FORTRAN IV program for interpolating irregularly spaced data using the difference equations for minimum curvature, *Comput. & Geosci.*, *1*(4), 231-240.

Tong, X., D. T. Sandwell, and B. Smith-Konter (2013), High-resolution interseismic velocity data along the San Andreas Fault from GPS and InSAR, J. Geophys. Res.; Solid Earth, 118, doi:10.1029/2012JB009442.

Tong, X., B. Smith-Konter, and D. T. Sandwell (2014), Is there a discrepancy between geological and geodetic slip rates along the San Andreas Fault System?, *J. Geophys. Res. Solid Earth, 119*, doi:10.1002/2013JB010765.

Wei, M., D. T. Sandwell, and B. Smith-Konter, Optimal combination of InSAR and GPS for measuring interseismic crustal deformation, *J. Adv. in Space Res.* doi:10.1016/j.asr.2010.03.013, 2010.

Wessel, P., and D. Bercovici (1998), Interpolation with splines in tension: a Green's function approach, *Math. Geol.*, *30*(1), 77–93, doi:10.1023/A:1021713421882.

Wessel, P., W. H. F. Smith, R. Scharroo, J. F. Luis, and F. Wobbe (2013), Generic Mapping Tools: Improved version released, *Eos Trans. AGU*, *94*(45), 409–410, doi:10.1002/2013EO450001.